MARTIN MARIETTA ENERGY SYSTEMS LIBRARIES
3 4456 0149630 6

OAK LABORATORY

UNION CARBIDE CORPORATION
for the
U.S. ATOMIC ENERGY COMMISSION

ORNL-TM-2221

COPY NO. - 29

DATE - June 24, 1968

Neutron Physics Division

NEUTRON FLUX AND NEUTRON AND GAMMA-RAY SPECTRA MEASUREMENTS AT THE HFIR

T. V. Blosser and G. E. Thomas, Jr.*

ABSTRACT

Preliminary neutron flux and neutron and gamma-ray spectra measurements were made at the exit of the High Flux Isotope Reactor (HFIR) beam tubes HB-2 (radial beam tube) and HB-3 (tangential beam tube) to determine the effect of the location of the beam tube on the emerging radiation. A comparison of the neutron flux at various energies showed a variation between HB-2 and HB-3 of from about 11% at thermal energies to a factor of 10.2 at 6.3 MeV.

There is a marked difference between the gamma-ray spectrum that each beam tube exhibits.

OAK RIDGE NATIONAL LABORATORY
CENTRAL RESEARCH LIBRARY
CIRCULATION SECTION
4500N ROOM 175
LIBRARY LOAN COPY
DO NOT TRANSFER TO ANOTHER PERSON.
If you wish someone else to see this report, send in name with report and the library will arrange a loan.
ORNL-118 (6-97)

*Argonne National Laboratory, Physics Division

NOTICE This document contains information of a preliminary nature and was prepared primarily for internal use at the Oak Ridge National Laboratory. It is subject to revision or correction and therefore does not represent a final report.

LEGAL NOTICE

This report was prepared as an account of Government sponsored work. Neither the United States, nor the Commission, nor any person acting on behalf of the Commission:

A. Makes any warranty or representation, expressed or implied, with respect to the accuracy, completeness, or usefulness of the information contained in this report, or that the use of any information, apparatus, method, or process disclosed in this report may not infringe privately owned rights; or

B. Assumes any liabilities with respect to the use of, or for damages resulting from the use of any information, apparatus, method, or process disclosed in this report.

As used in the above, "person acting on behalf of the Commission" includes any employee or contractor of the Commission, or employee of such contractor, to the extent that such employee or contractor of the Commission, or employee of such contractor prepares, disseminates, or provides access to, any information pursuant to his employment or contract with the Commission, or his employment with such contractor.

INTRODUCTION

It was proposed that preliminary neutron flux and neutron and gamma-ray spectra measurements be made at the HFIR in beam holes HB-2 (radial beam tube) and HB-3 (tangential beam tube) to furnish experimental information for ORNL and to aid in the conceptual design of the beam tubes for the ANL Advanced Research Reactor. To utilize the reactor operating time efficiently, the measurements were made while the low-power operation tests were being made.

The neutron flux and the spectra measurements were made in order to determine the effect of the beam tube orientation in the reactor on the emerging neutron radiation. Figure 1 shows the orientation of the beam tubes in respect to the reactor core at the horizontal midplane.

To obtain a comparison between HB-2 and HB-3 over a large range of neutron energies, several types of foil detectors were used to measure the thermal, resonance, and fast-neutron fluxes.

Measurements of the gamma-ray energy spectrum and relative intensity were made in both beam tubes before the reactor had been operated at a significant power level (1-3 W) for any appreciable length of time. It was desirous to make these measurements with a cold reactor rather than one operated at a high-power level in order to measure the fission and capture gamma-ray spectrum produced in the reactor core instead of the gamma-ray activity produced in the structural material of the reactor.

Comparison of the resonance neutrons (epithermal) which was made from 0.325 eV to 5 keV using the ^{10}B absorption technique will be reported later.

MARTIN MARIETTA ENERGY SYSTEMS LIBRARIES
3 4456 0149630 6

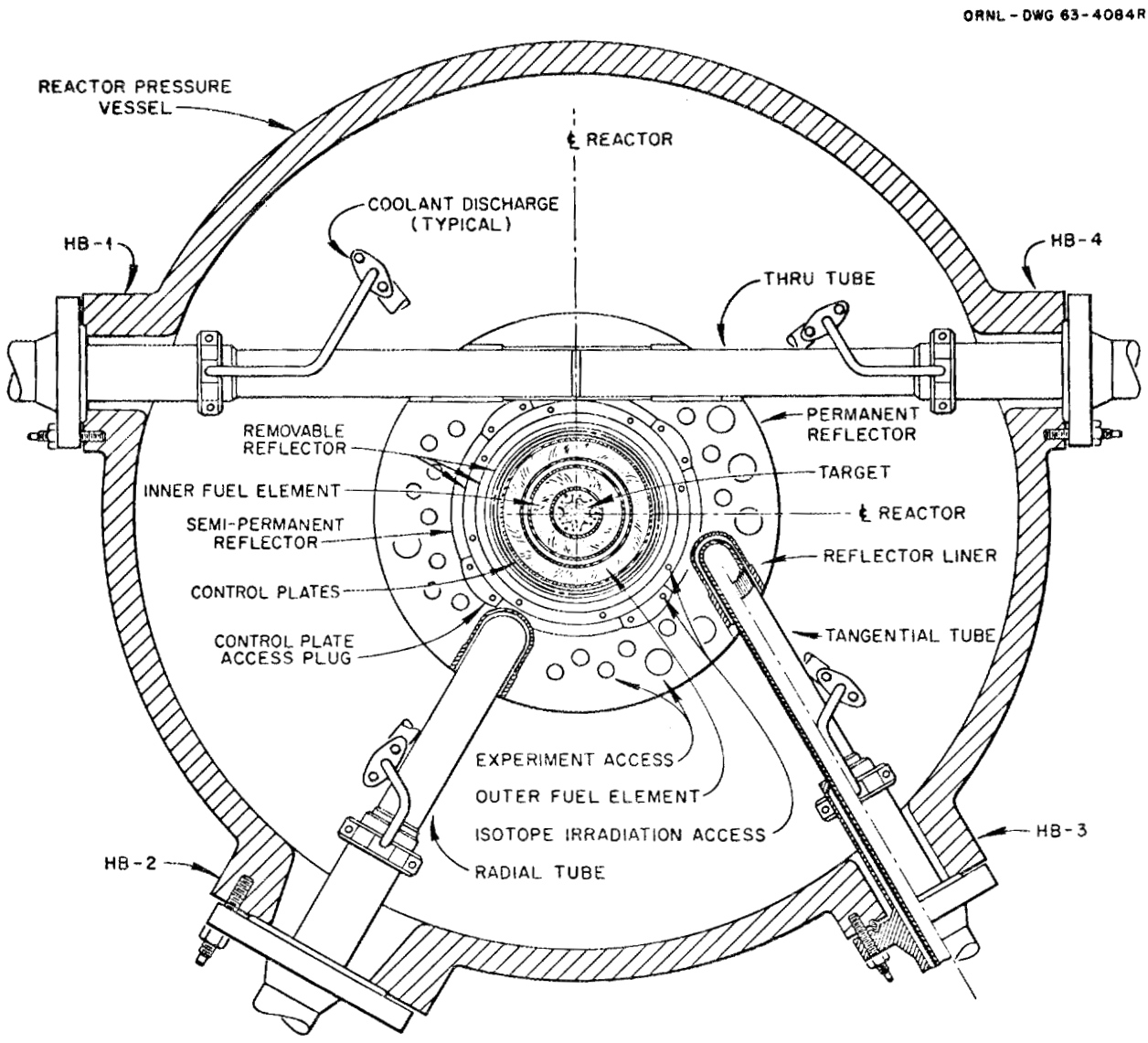

Fig. 1. Cross Section of Reactor Core at the Horizontal Midplane Showing the Orientation of the Beam Tubes in the Reactor Core.

Experimental Arrangement

The experiments were designed so that the measurements could be made simultaneously in both beam holes at the same reactor power level. This required collimators and shutter openings of different sizes to produce neutron and gamma-ray beam intensities suitable for the type of detector being used.

The shutter and collimator arrangement is shown in Fig. 2. The collimators were designed so that they would fit either beam tube, which allowed a given collimator-shutter opening arrangement to be used as the experiment dictated. For the high-intensity beam, the shutter opening was 3.5 in. in diameter, and for the low-intensity beam, it tapered from 0.234 in. in diameter to 1 in. in diameter; in both cases the length of the beam tube from the shutter to the detector position was 6 ft, and an air gap of 6 in. existed between the shutter and the leading edge of the beam tube.

The low-intensity beam terminated in a 3- by 2- by 2-ft-cavity beam catcher in which the detectors were placed. In the high-intensity beam, a cross-slide was mounted on the end of the beam tube for personnel safety in placing the foil detectors. Approximately 3 ft from the cross-slide the beam terminated in a water-filled tank 6.5 ft in diameter and 6.5 ft high. This tank also served as a suitable place to make beam-scattering experiments on various materials.

Foil Detectors

Several types of foils were used to measure the thermal, resonance, and fast-neutron flux. Generally, the foils selected have simple decay schemes, emit particles that are energetic, and have a half-life conducive

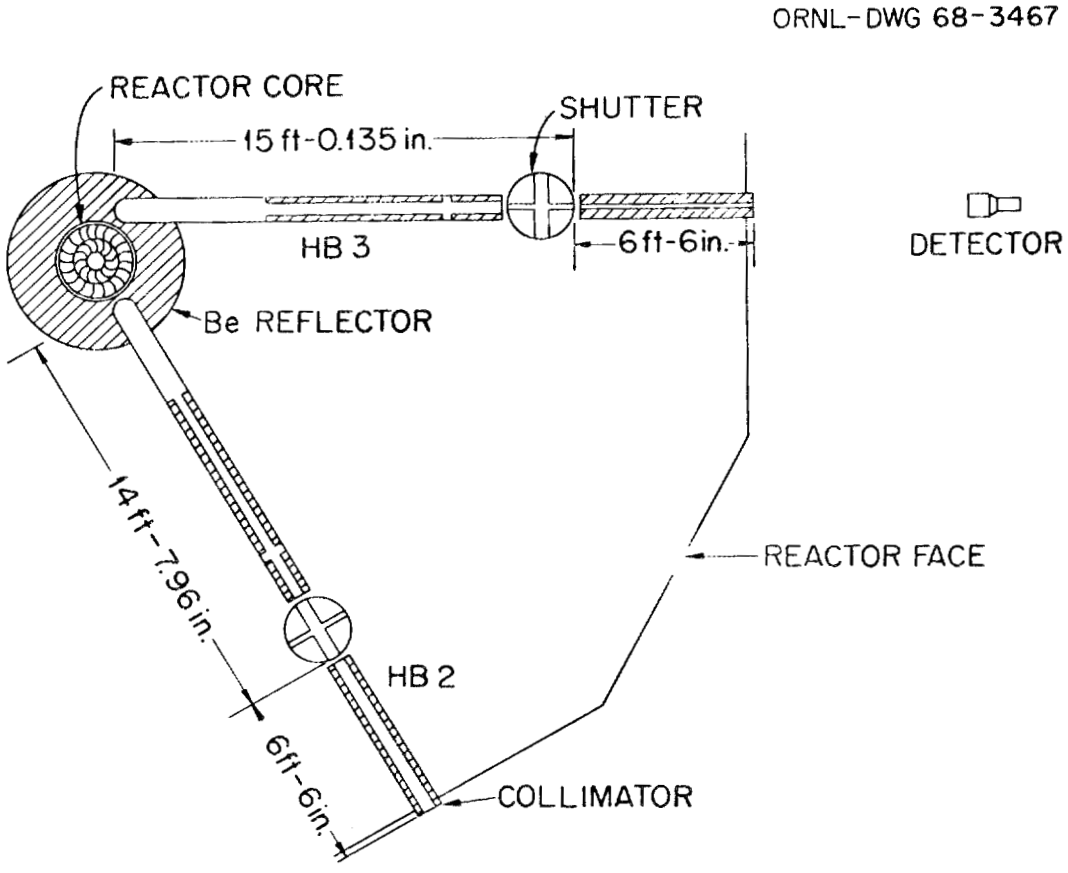

Fig. 2. Schematic of the Collimator and Shutter Arrangement in HB-2 and HB-3.

for simple counting techniques.

The thermal and resonance neutron foil detectors were made thin so that the self-shielding factor for thermal neutrons would be small. The thin foils also satisfied the infinite dilution approach for measuring the "effective resonance integral," which is used in the cadmium-difference method for determining the resonance neutron flux. All the foils with the exception of the sodium and sulfur were prepared from highly pure metal and were 1.25 in. in diameter. The sodium foils were prepared from sodium carbonate (Na_2CO_3) which was pressed into a Lucite cylinder 1.25 in. in outside diameter. The wall thickness of the Lucite cylinder was 3 mils; the combined thickness of the Lucite cylinder and sodium pellet was 40 mils. The sulfur was triply distilled and molded into pellets 1.5 in. in diameter and 0.375 in. thick.

Reaction data for the detectors are given in Table 1; the thermal-neutron self-shielding factors for the foils are given in Table 2.

Foil Counting Equipment

All foils with the exception of the sulfur were counted on a two-crystal NaI counter.[1] The sulfur foils were placed in a specially prepared 0.5-mil aluminum cup and burned. The burned residue, which contained ^{32}P, was counted on an NE-102 crystal counter. The counters were calibrated by comparison to either a known neutron flux in the Standard Pile or a standard high-pressure ion chamber.

NEUTRON FLUX MEASUREMENT

The term "thermal flux" implies a Maxwellian distribution of velocity and energy corresponding to the most probable velocity of 2200 m/sec at ~293.4°K. This assumption for the thermal flux appears reasonable for

Table 1. Reaction Data for Thermal, Resonance, and Threshold Detectors

Reaction	Half-Life	Effective Threshold (MeV)	Cross Section (barns)
	Thermal and Resonance Detectors		
$^{23}Na(n,\alpha)^{24}Na$	15 h	Thermal	0.536 ± 0.010[a]
$^{63}Cu(n,\alpha)^{64}Cu$	12.82 h	Thermal	4.3 ± 0.2[a]
$^{59}Co(n,\alpha)^{60}Co$	5.29 y	Thermal	37.0 ± 1.5[a]
$^{115}In(n,\alpha)^{116}In$	54.2 m	Thermal	155.0 ± 10[a]
$^{197}Au(n,\alpha)^{198}Au$	2.7 d	Thermal	96.0 ± 10[b]
	Threshold Detectors		
$^{239}Pu(n,f)$		0.003 - 0.005	1.94[c]
$^{237}Np(n,f)$		0.75	1.6[c]
$^{238}U(n,f)$		1.4	0.525[c]
$^{32}S(n,p)^{32}P$	14.3 d	2.9	0.300
$^{27}Al(n,p)^{27}Mg$	9.8 m	4.6	0.039
$^{24}Mg(n,p)^{24}Na$	1.5 h	6.3	0.048
$^{27}Al(n,\alpha)^{24}Na$	15 h	8.1	0.110

[a]From: D. J. Hughes and J. A. Harvey, Neutron Cross Sections, BNL-325 (1958); also Supplement 1 (1960).

[b]98 barns is the value suggested in BNL-325.

[c]Flux measurements using these reactions were made (by G. W. Main, ANL) with a fission counter.

Table 2. Foil Description

Detector	Thickness (mils)	Thermal-Neutron Self-Shielding Factor
Sodium	12	0.99
Copper	5	0.99
Cobalt	10	0.96
Indium	0.4	0.99
Gold	0.2	0.99
Sulfur	375	
Magnesium	9	
Aluminum	20	

the measurements since the temperature of the neutrons at the detector position is not known.

Measurements of the thermal flux were made by the cadmium-difference method with the thermal detectors listed in Table 1. The method of cadmium difference requires that the foil detector be thin so that the self-shielding and perturbation of the 1/v neutrons are small. The foil detectors were encased in 20-mil-thick cadmium covers. In a beam geometry this thickness of cadmium is just sufficient to remove the thermal neutrons and to minimize the attenuation of the epithermal neutrons.

The detectors were placed in the 3.5-in.-diam beam by a cross-slide attached to the end of the collimator. The detector holder was made from a 0.0625-in.-thick aluminum plate. To minimize neutron backscattering, a hole having the same diameter (1.25 in.) as the foil was

made in the plate on the beam's central axis, into which the foils were placed for irradiation. The saturated activity of each pair of foils was normalized for isotopic weight and a reactor power level of 1 MW.

The following equation was used to compute the neutron flux φ, which is in units of neutrons cm^{-2} sec^{-1}:

$$\varphi = \frac{M\lambda C}{N\bar{\sigma}W\epsilon\,(1 - e^{-\lambda t_1})\,(1 - e^{-\lambda t_2})\,e^{-\lambda t_3}} \quad , \qquad (1)$$

where

M = atomic weight of target isotope,

λ = disintegration constant of the product isotope,

C = net counts for time t_2,

N = Avogadro's number,

$\bar{\sigma}$ = activation cross sections at 2200 m/sec/1.128,

W = weight of target isotope,

ϵ = counter efficiency for product isotope,

t_1 = irradiation time,

t_2 = count time,

t_3 = decay time (end of irradiation to beginning of count time).

The thermal fluxes, foil activities, and cadmium ratios for the foil detectors are given in Table 3. The thermal-neutron data for the cobalt foils have been corrected for the thermal-flux depression in both cases.

RESONANCE-NEUTRON FLUX

The same foil detectors were used to make the resonance-neutron-flux measurements that were used in determining the thermal flux. To eliminate the thermal-flux activation produced in the foil, 20-mil-thick

cadmium covers were used to encase the foil. With this thickness of cadmium placed in a moderated beam of reactor neutrons, a reasonable assumption for the lower energy cutoff would be about 0.4 eV. The variation of this assumed value of energy cutoff has been determined by calculation as well as by experiment.[2-4]

If one defines the ratio of the saturated activity of the bare foil A^B to that of the cadmium-covered foil A^{cd} as the cadmium ratio R^{cd}, then

$$\frac{A^B}{A^{cd}} - 1 = R^{cd} - 1 \quad . \tag{2}$$

Table 3. Thermal Flux, Foil Activities, and Cadmium Ratios of the Various Detectors Used in Beam Tubes HB-2 and HB-3

Foil	Foil Activity (neutrons cm^{-2} sec^{-1}) Bare Foil	Cadmium-Covered Foil	Thermal Flux (neutrons cm^{-2} sec^{-1})	Cadmium Ratio
		Beam Tube HB-2		
Au	1.076×10^8	3.488×10^7	7.633×10^7*	3.0846
Cu	7.783×10^7	3.423×10^4	7.779×10^7	2273.7
In	1.168×10^8	3.915×10^7	7.765×10^7	2.983
Co	7.913×10^7	4.246×10^6	7.487×10^7	18.63
Na	7.845×10^7	2.461×10^6	7.6×10^7	31.87
		Av.	7.652×10^7	
		Beam Tube HB-3		
Au	1.020×10^8	3.323×10^7	6.877×10^7	3.071
Au	1.037×10^8	3.424×10^7	6.946×10^7	3.029
Cu	6.893×10^7	2.210×10^4	6.890×10^7	3119
In	9.693×10^7	3.204×10^7	6.489×10^7	3.025
Co	7.061×10^7	3.534×10^6	6.987×10^7	19.984
Na	7.109×10^7	1.710×10^6	6.938×10^7	41.59
		Av.	6.870×10^7	

*Corrected for flux perturbation.

From the cadmium ratio it can be shown that

$$R^{cd} - 1 = \frac{\varphi_{th}\ \sigma_{th}}{\int_{0.4\ eV}^{\infty} \varphi(E)\ \sigma_a(E)\ dE} = \frac{\text{thermal response}}{\text{epicadmium response}}, \qquad (3)$$

where

φ_{th} = thermal flux at 2200 m/sec,

σ_{th} = foil cross section at 2200 m/sec,

σ_a = absorption cross section,

E = neutron energy.

In a neutron slowing-down spectrum which has a 1/E distribution, $\varphi(E)$ can be represented by K/E, where K is a constant; then

$$K = \frac{\varphi_{th}\ \sigma_{th}}{R^{cd} - 1 \int_{0.4\ eV}^{\infty} \sigma_a \frac{dE}{E}} = E\ \varphi(E). \qquad (4)$$

A measurement of K involved the determination of R^{cd}, the thermal-neutron flux, and the cross section and a knowledge of the resonance integral. The resonance activation integral is represented by

$$\text{resonance integral} = \int_{0.4\ eV}^{\infty} \sigma_a \frac{dE}{E}. \qquad (5)$$

However, the resonance integral is the sum of two parts, the 1/v (v = neutron velocity) contribution plus the resonance contribution:

$$\int_{0.4\ eV}^{\infty} \sigma_a \frac{dE}{E} = \int_{0.4\ eV}^{\infty} \sigma_{(\frac{1}{v})} + \int_{0.4\ eV}^{\infty} \sigma_{(res)} \frac{dE}{E}. \qquad (6)$$

The ratio of the two parts may be defined as

$$\alpha = \frac{\int_{0.4\,eV}^{\infty} \sigma_{(res)} \frac{dE}{E}}{\int_{0.4\,eV}^{\infty} \sigma_{(\frac{1}{v})} \frac{dE}{E}} = \frac{\text{resonance activation}}{\frac{1}{v}\text{ activation}} , \tag{7}$$

$$\int_{0.4\,eV}^{\infty} \sigma_{(res)} \frac{dE}{E} = \alpha \int_{0.4\,eV}^{\infty} \sigma_{(\frac{1}{v})} \frac{dE}{E} . \tag{8}$$

For a foil having a pure 1/v activation cross section when placed in a 1/E type flux, it can be shown that the thermal cross section is approximately twice the activation integral, or

$$\int_{0.4\,eV}^{\infty} \sigma_{(\frac{1}{v})} \frac{dE}{E} \cong 0.5\ \sigma_{th} . \tag{9}$$

Experimentally, however, when applying corrections of neutron temperature and the cadmium-cover factors, the activation integral is about 0.44 σ_{th}.[5] When rearranging the quantities of α and 0.44 σ_{th} into Eq. (4) it becomes

$$K = \frac{2.27\ \varphi_{th}}{(R^{cd} - 1)\ (1 + \alpha)} = E\ \varphi(E) , \tag{10}$$

where $E\ \varphi(E)$ = resonance flux per ln e interval.

The differential neutron flux in the region of the resonance would be as follows:

$$\frac{E\ \varphi(E)}{E} = \varphi(E)[\text{neutrons cm}^{-2}\ \text{sec}^{-1}(\text{energy interval})^{-1}] . \tag{11}$$

The foil resonance parameters and values computed for alpha are shown in Table 4, and the values of $E\varphi(E)$ and $\varphi(E)$ for the selected resonance detectors are shown in Table 5. From Eq. (4) if a 1/E spectral distribution exists, $E\varphi(E)$ will be constant. The values of $E\varphi(E)$ in beam hole HB-2 appear, within experimental errors, to be constant from an energy of 1.45 eV(^{115}In measurements) through 132 eV (^{59}Co measurements). It would then be justifiable to assume a 1/E spectral response over this energy region. The ^{23}Na detector value of $E\varphi(E)$ indicates that a 1/E spectral distribution does not exist in this region.

Within the experimental errors of the measurements made in beam hole HB-3, a 1/E spectral distribution exists throughout the energy range from 1.45 through 2850 eV.

FAST-NEUTRON FLUX

The spectrum in the neutron energy region from about 3 keV through approximately 1 MeV was measured by E. R. Bennett, ANL, with a proton-recoil proportional counter. His measurements will be reported[6] with all the nuclear data taken in the beam tubes.

Table 4. Resonance Parameters

Element	Resonance Energy[a] (eV)	Resonance Activation Integral[b] (barns)	Alpha
^{23}Na	2850	0.24	0.900
^{59}Co	132	49.3	2.716
^{115}In	1.46	2640	34.06
^{197}Au	4.9	1588	32.40

[a] From D. J. Hughes and J. A. Harvey, Neutron Cross Sections, BNL-325 (1958); also Supplement 1 (1960).

[b] From ref. 5.

Table 5. Values of $E\,\varphi(E)$ and $\varphi(E)$ Determined in Beam Tubes HB-2 and HB-3

Element	Cadmium Ratio	$E\,\varphi(E)$	$\varphi(E)$ (neutrons cm^{-2} sec^{-1} MW^{-1})
		HB-2	
^{115}In	2.984	2.534×10^6	1.735×10^6
^{197}Au	3.085	2.485×10^6	5.07×10^5
^{59}Co	17.93	2.583×10^6	1.92×10^4
^{23}Na	31.87	2.949×10^6	1.04×10^3
		HB-3	
^{115}In	3.025	2.072×10^6	1.42×10^6
^{197}Au	3.071	2.258×10^6	4.61×10^5
^{59}Co	19.98	2.256×10^6	1.67×10^4
^{23}Na	41.59	2.049×10^6	7.19×10^2

The theory of determining fast-neutron flux with threshold detectors is discussed by Hughes,[2] Trice,[7] Hurst,[8] Uthe,[9] Grundle and Usner,[10] and Grundle.[11] Each one used various methods of interpreting the spectral distribution derived from a given number of detector response integrals. The most simple and easiest method to apply is discussed by Hughes[2] and applied by Hurst[8] and Trice.[7] In this method the cross section of the detector is assumed to be a step function characterized by its effective cross section σ_{eff} and corresponding threshold energy E_{eff} values as determined for a fission spectrum.

The saturated activity A induced in the detector is

$$A = N \int_0^\infty \sigma(E)\, \varphi(E)\, dE \ ,$$

where N = total number of target nuclei in the detector, $\sigma(E)$ = the differential cross section for the reaction in consideration, $\varphi(E)$ = the fast flux density per unit of energy interval, and E = neutron energy. If $\varphi(E)$ is a known function of energy, such as that of the fission

spectrum, then the equation becomes

$$A = N\,\sigma_{eff} \int_{E_{eff}}^{\infty} \varphi(E)\,dE = \Phi(E_{eff}),$$

where $\Phi(E_{eff})$ is the integral flux above E_{eff}. If the actual neutron spectrum differs appreciably from the fission spectrum, the use of the method will produce errors in the result.

The fast-neutron flux data measured in beam holes HB-2 and HB-3 are shown in Table 6. The data have been normalized to a reactor power level of 1 MW. Obviously, for a good insight of the spectrum several detectors with appropriately chosen thresholds are needed. A comparison of the integral flux measurements of HB-2 and HB-3 shows a variation as large as a factor of 10.2 for the 6.3-MeV threshold detector. However, this increase in neutron flux is to be expected since HB-2 "views" the reactor core.

DISCUSSION OF RESULTS

The accuracy of a given neutron flux is dependent primarily on the accuracies of the counting efficiency of the related foil, the activation cross section of the target isotope, and the reactor power level at the time of irradiation.

The overall accuracy for determining the activity of the foils is about ±6%. This error includes the ±2% counting statistics, the irradiation exposure time, and a ±2 to 5% counter efficiency error for a given isotope. The counter efficiency for a given isotope was determined by irradiating the foil in the standard pile in a known thermal neutron flux, which was corrected for flux perturbation due to the presence of the foil. The accuracy of the activation cross section for a given foil varies from a few percent to ±10% as shown in Table 1.

The reactor was operated at a power level of between 16 and 18 MW. It was estimated by the Reactor Operations Division that the power at this level could be determined to within ±1 MW. This error in the reactor power would cause an error in the measurements of about ±6%. The total accumulated errors of the measurements would then be approximately ±13 to 14%.

Neutron flux measurements at various neutron energies are compared in Table 7. The results are reported as the type of flux a given detector measures; that is, for thermal neutrons it is a Maxwellian distribution, for epithermal neutrons it is the flux per unit energy interval, and for fast neutrons it is the integral fast flux above a given energy threshold.

GAMMA-RAY SPECTRUM MEASUREMENTS

It was desirous to make the gamma-ray spectrum measurements at low power levels with a cold reactor so that the spectrum observed would more closely represent the gamma rays emitted by the reactor core and not the gamma rays produced by the activated materials in the proximity of the reactor core. The low reactor power level allowed the use of a 3- by 3-in. NaI scintillation detector to view the direct beam being emitted in each beam tube. So as not to activate the NaI by neutrons from the beam, a ^{6}Li shield was placed around the detector when the spectrum measurements were being made. After the low-power measurement was completed, several measurements were repeated with the ^{6}Li shield removed to determine whether there was an appreciable difference between the two spectra.

Table 6. Fast-Neutron Flux Measurement in Beam Holes HB-2 and HB-3.

Reaction	Threshold Energy (MeV)	$\varphi(E_{eff})$ (neutrons $cm^{-2}sec^{-1}MW^{-1}$) HB-2	HB-3
$^{32}S(n,p)^{32}P$	2.9	3.72×10^6	7.93×10^5
$^{24}Mg(n,p)^{24}Na$	6.3	1.25×10^6	1.23×10^5
$^{27}Al(n,\alpha)^{24}Na$	8.1	2.04×10^5	2.62×10^4

Table 7. Comparison of Neutron Flux Measurements at Various Neutron Energies.

Energy (eV)	Neutron Flux (neutrons $cm^{-2}sec^{-1}MW^{-1}$) HB-2	HB-3	Ratio
Thermal	7.64×10^7	6.87×10^7	1.11
Epithermal			
1.46	1.735×10^6	1.42×10^6	1.22
4.9	5.07×10^5	4.61×10^5	1.10
132	1.92×10^4	1.67×10^4	1.15
2850	1.04×10^3	7.19×10^2	1.44
Fast-Neutron			
2.9×10^6	3.73×10^6	7.93×10^5	4.70
6.3×10^6	1.25×10^6	1.23×10^5	10.22
8.1×10^6	2.00×10^5	2.61×10^4	7.66

The experimental facility as shown in Fig. 2 depicts two separate collimation systems that can be interchanged between the beam ports. The figure illustrates a tapered collimator mounted in beam hole HB-3, which produces almost a point source at the reactor core position and enlarges to ~ 3 in. at the detector position. The other collimator configuration, shown in HB-2, produces a straightthrough beam ~3.25 in. in diameter. Both collimator configurations were used at each beam hole in making the spectral measurements.

A 3- by 3-in. NaI scintillation detector was chosen to measure the spectrum because of its sensitivity and because its characteristics, such as gamma-ray efficiency as a function of energy, have been thoroughly measured.[12]

The detector system was calibrated before and after making spectral measurements using the following gamma-ray sources: ^{198}Au, ^{137}Cs, ^{60}Co, ^{24}Na, and Po-Be. A measure of the stability of the system is the good agreement of the separate calibration runs. The energy calibration curves used with these spectral measurements are shown in Fig. 3. A conventional preamplifier and amplifier were used with a 400-channel analyzer to make the measurements. A pulser was used to determine the linearity of the system over the full 400-channel range. The detector was shielded with a sufficient thickness of concrete blocks and lead so that the room background made a negligible contribution to the spectra measurements.

Measurements were made at power levels of 3, 30, and 90 W. It was difficult to determine accurately the low 3-W power level, and a beam monitor was used to normalize all three power levels. However, it was

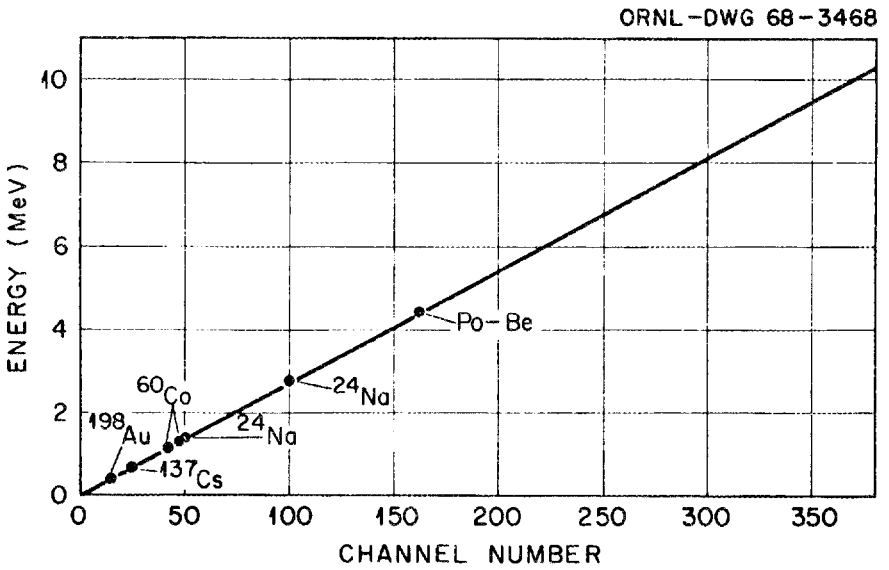

Fig. 3. Energy Calibration Curves Obtained with NaI Scintillation Detector.

found that all three power levels gave similar spectra; therefore only the 3- and 90-W spectra are shown for each beam tube.

The results of the radial beam hole spectrum measurements at both 3 and 90 W are shown in Figs. 4 and 5. The live times of each run are given with Figs. 4-6 so that an absolute comparison of the different spectra may be made if so desired. Since the radial beam hole looks directly at the reactor core and also views a large amount of aluminum, one would expect to see the aluminum capture gamma rays and also fission gamma rays. This is verified by the identification of the aluminum line at 7.24 MeV and also the high continuum in the spectrum at energies up to 6-7 MeV. This continuum is particularly noticeable when compared with that of the tangential beam port. Although there is a relatively small amount of beryllium in the beam, it is felt that these lines are not seen as they are masked out both by the fission continuum and the intensity of the aluminum lines.

The spectrum from the tangential beam hole measurements is shown in Figs. 6 and 7. The location of the beam tube (see Fig. 2) is such that the beam tube does not view the reactor core but looks directly at the beryllium reflector, as well as at a considerable amount of aluminum. As a result, the lines in the spectra from aluminum (7.72 MeV) and beryllium (6.84 and 3.37 MeV) are quite readily resolved. Also, because of the lack of gamma rays from fission neutrons, the continuum below 6-7 MeV as previously mentioned is much less in the radial beam. This makes it easier to see lower energy gamma rays, such as the beryllium (3.37 MeV) and sodium (1.37 and 2.76 MeV) background lines, equally well at both power levels. In both the tangential and radial beam spectra

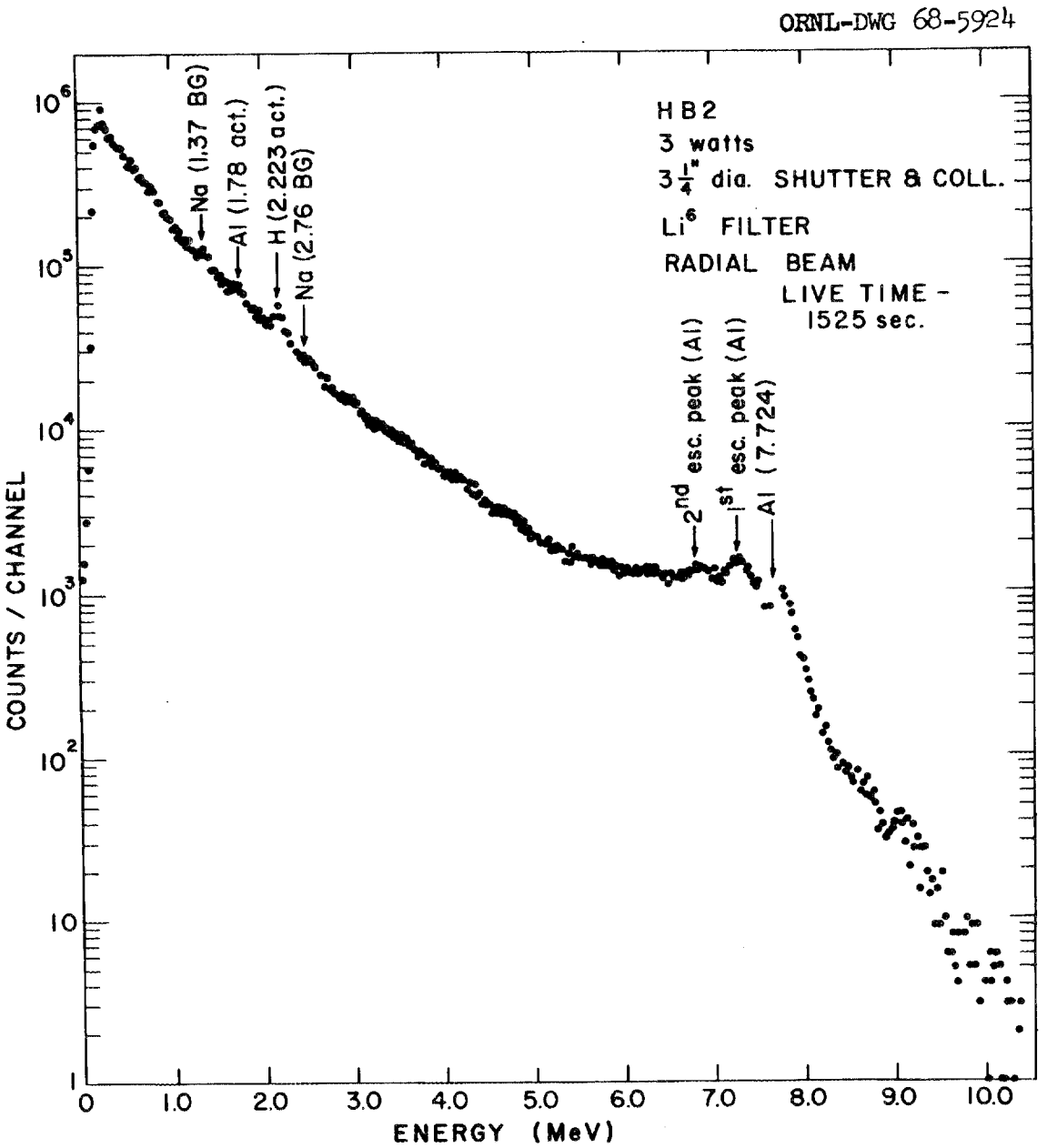

Fig. 4. Gamma-Ray Spectrum in HB-2 at 3 W.

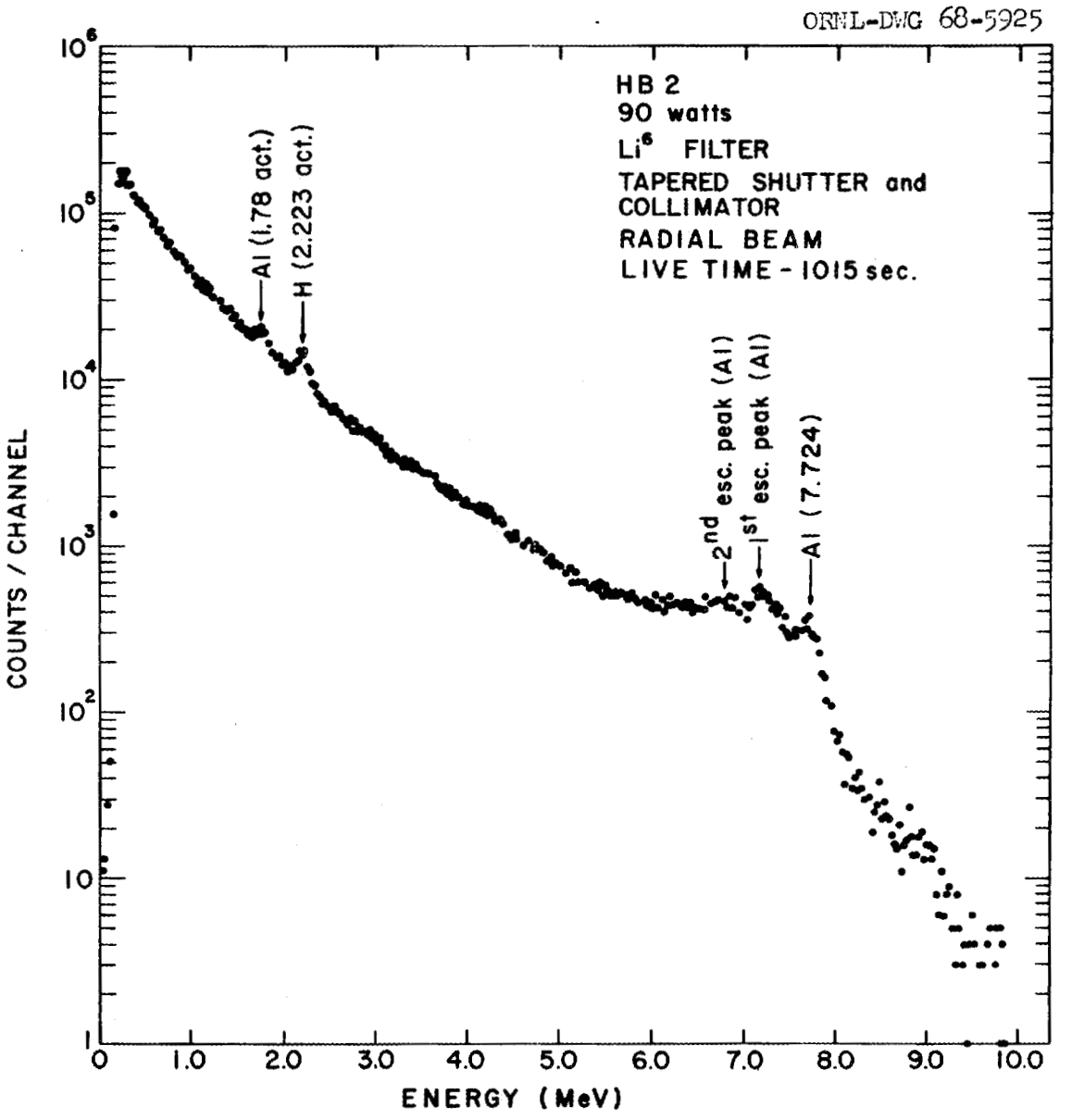

Fig. 5. Gamma-Ray Spectrum in HB-2 at 90 W.

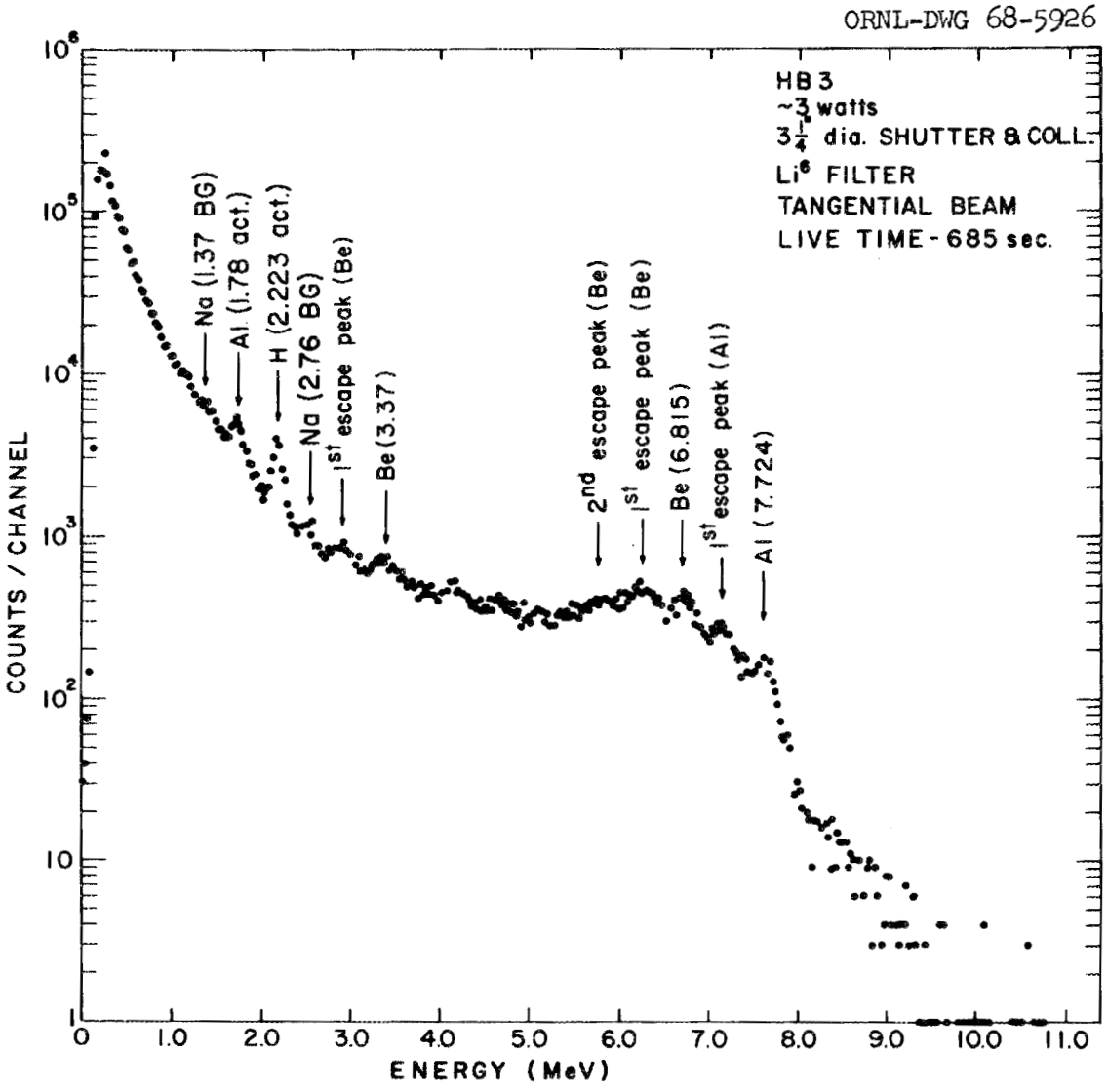

Fig. 6. Gamma-Ray Spectrum in HB-3 at 3 W.

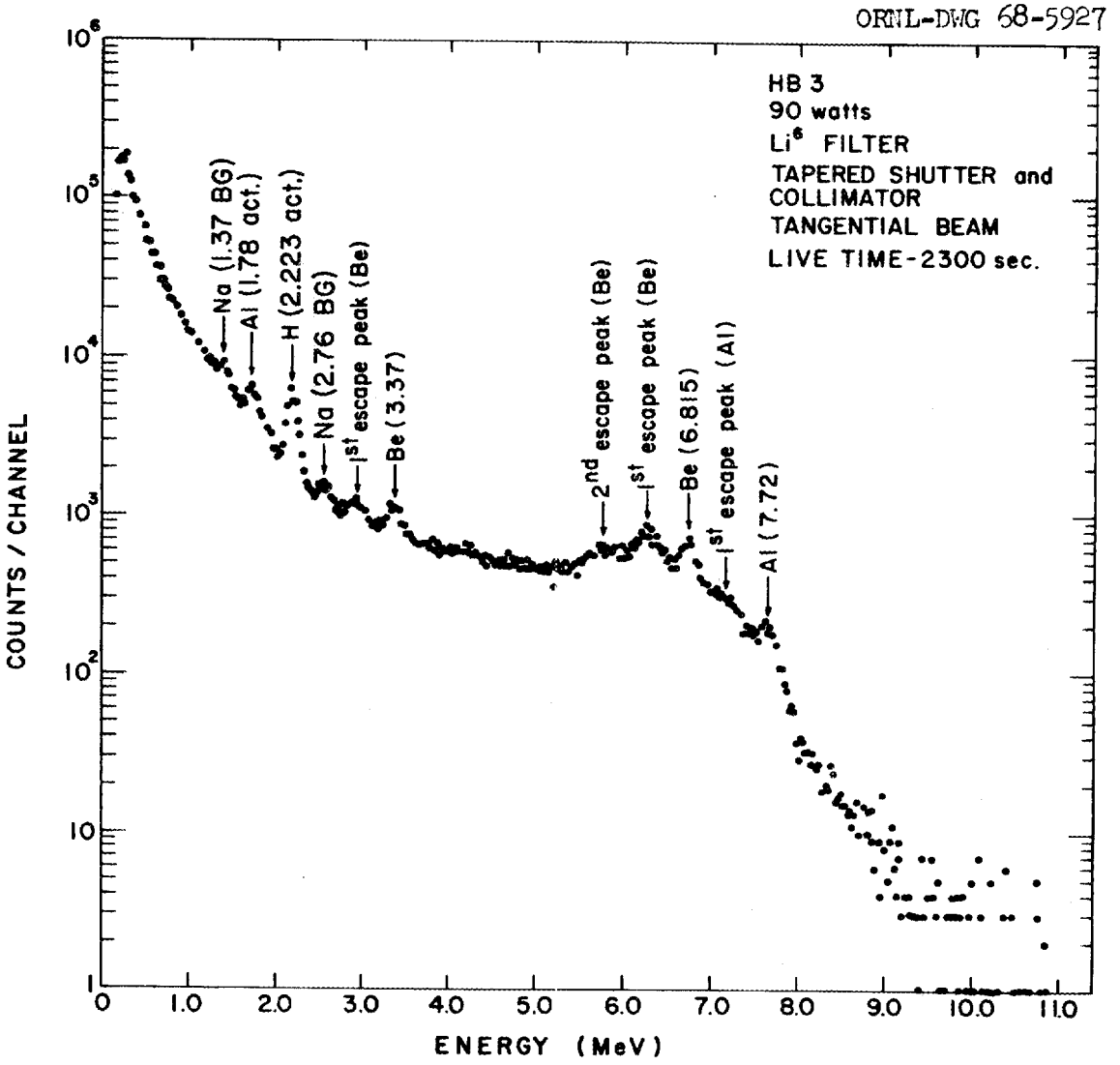

Fig. 7. Gamma-Ray Spectrum in HB-3 at 90 W.

the hydrogen (2.23 MeV) line was produced from the water in the reactor. Other lines in middle-energy regions of the spectra might have been resolved with better statistics by using a Ge-Li detector.

Some of the peaks in Figs. 4-7 have been identified as spectra lines which resulted from the background as shown in Fig. 8. The sodium lines probably represent the activation of the NaI crystal by epithermal neutrons in the beam that were transmitted through the ^{6}Li filter, with some of the activation probably resulting from the low-power runs when the ^{6}Li filter was not used.

GAMMA-RAY DOSE MEASUREMENTS

Gamma-ray dose measurements were made in HB-2 and HB-3 beam tubes using the 3.5-in.-diam shutter opening and beam tube arrangement as previously described. The calibrated ionization chambers (Victoreen Model 570) were exposed in the beam for a given period of time, and the ionization was recorded. The estimated dose at 1 MW for HB-2 was 2.1×10^{3} r/hr and for HB-3 was 217 r/hr. The ratio between HB-2 and HB-3 is approximately 9:1.

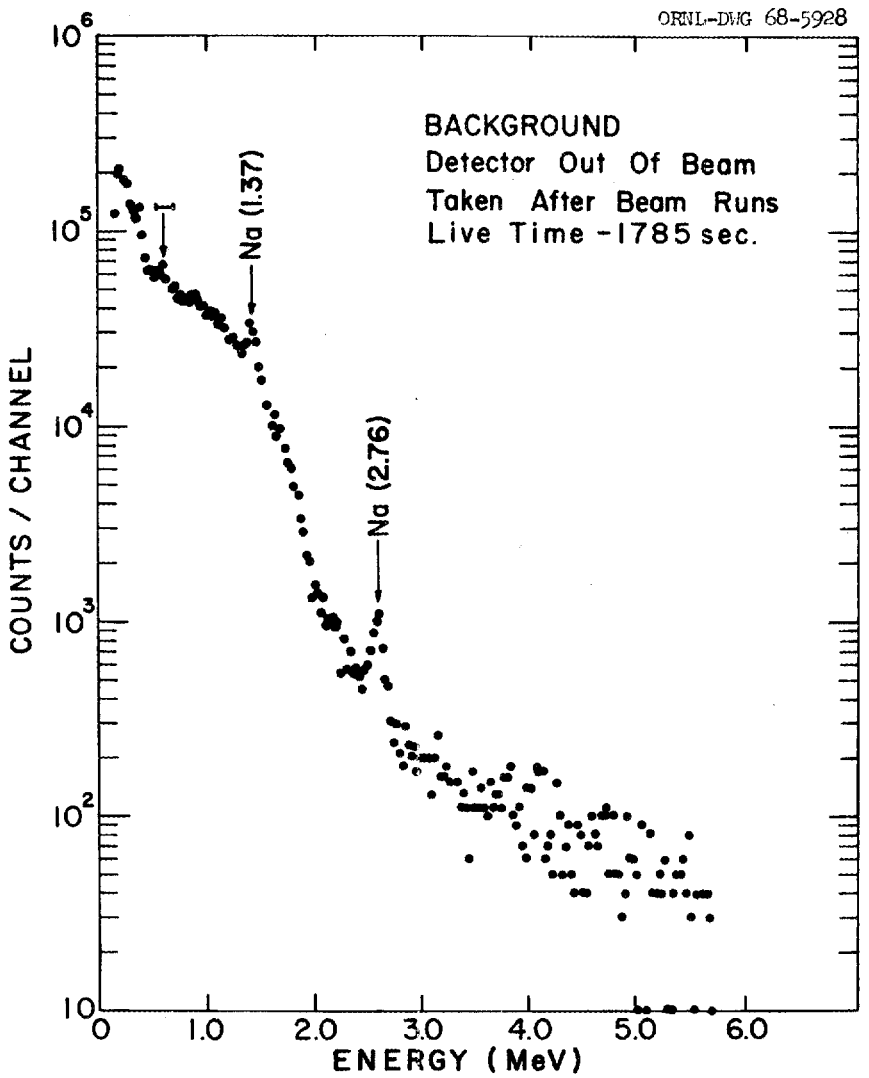

Fig. 8. Gamma-Ray Background.

ACKNOWLEDGMENTS

The authors wish to acknowledge D. W. Conner (ANL Solid States Science Division), who initiated and planned the experiment with the assistance of G. R. Ringo (ANL Physics Division); F. C. Maienschein (ORNL Neutron Physics Division) for helpful suggestions during the experiment; C. Cagle, R. V. McCord, R. A. Costner, Jr., and T. E. Cole, who represented the ORNL HFIR operation in charge of administrative liaison; and O. W. Christian, H. Todd, and C. McNew (ORNL Neutron Physics Division) and J. R. Specht (ANL Physics Division), who aided in performing the experiments.

REFERENCES

1. T. V. Blosser and D. K. Trubey, Neutron Phys. Div. Ann. Progr. Rept. Sept. 1, 1960, ORNL-3016, p. 142.

2. D. J. Hughes, Pile Neutron Research, Addison-Wesley, Cambridge, Mass., 1953.

3. R. W. Stoughton, J. Halperin, and M. P. Lietzke, Effective Cadmium Cutoff Energies, ORNL-2823 (1960) and Supplement (1960).

4. I. E. Dalton and W. G. Pettus, Nucleonics 15(12), 86 (1957).

5. R. L. Macklin and H. S. Pomerance, Proc. Intern. Conf. Peaceful Uses At. Energy, Geneva, 1955 5, 96 (1955).

6. ANL Progress Report, to be published.

7. J. B. Trice et al., A Series of Thermal, Epithermal and Fast Neutron Measurements in MTR, ORNL-CF-55-10-140 (1955).

8. G. S. Hurst et al., Rev. Sci. Instr. 27, 153 (1956).

9. P. M. Uthe, Attainment of Neutron Flux Spectra Foil Activations, UCRL-5403 (1957).

10. J. A. Grundle and A. Usner, Nucl. Sci. Eng. 8, 598 (1960).

11. J. A. Grundle, Study of Fission Neutron Spectra with High-Energy Activation Detectors, LAMS-2883 (1963).

12. R. H. Heath, Scintillation Spectrometry Gamma-Ray Catalogue, IDO-16408 (July 1957).

INTERNAL DISTRIBUTION

1-3. L. S. Abbott
4. J. K. Baird
5-9. T. V. Blosser
10. A. Boch
11. C. D. Cagle
12. W. R. Casto
13. C. E. Clifford
14. T. E. Cole
15. R. A. Costner, Jr.
16. J. A. Cox
17. L. B. Holland
18-19. F. C. Maienschein
20. R. V. McCord
21. F. J. Muckenthaler
22. E. R. Cohen (consultant)
23. B. C. Diven (consultant)
24. W. N. Hess (consultant)
25. M. H. Kalos (consultant)
26. L. V. Spencer (consultant)
27-28. Central Research Library
29. Document Reference Section
30-44. Laboratory Records Department
45. Laboratory Records ORNL RC
46. ORNL Patent Office

EXTERNAL DISTRIBUTION

47. G. R. Ringo, Argonne National Laboratory, Argonne, Illinois
48. D. W. Conner, Argonne National Laboratory, Argonne, Illinois
49-53. G. E. Thomas, Jr., Argonne National Laboratory, Argonne, Illinois
54. P. B. Hemmig, Division of Reactor Development and Technology U. S. Atomic Energy Commission, Washington
55. I. F. Zartman, Division of Reactor Development, U. S. Atomic Energy Commission, Washington
56-70. Division of Technical Information Extension (DTIE)
71. Laboratory and University Division, ORO